LETTER

doi:10.1038/nature10111

A nuclear-receptor-dependent phosphatidylcholine pathway with antidiabetic effects

Jae Man Lee[1], Yoon Kwang Lee[2,3], Jennifer L. Mamrosh[2], Scott A. Busby[4], Patrick R. Griffin[4], Manish C. Pathak[5], Eric A. Ortlund[5] & David D. Moore[1,2]

Nuclear hormone receptors regulate diverse metabolic pathways and the orphan nuclear receptor LRH-1 (also known as NR5A2) regulates bile acid biosynthesis[1,2]. Structural studies have identified phospholipids as potential LRH-1 ligands[3–5], but their functional relevance is unclear. Here we show that an unusual phosphatidylcholine species with two saturated 12 carbon fatty acid acyl side chains (dilauroyl phosphatidylcholine (DLPC)) is an LRH-1 agonist ligand *in vitro*. DLPC treatment induces bile acid biosynthetic enzymes in mouse liver, increases bile acid levels, and lowers hepatic triglycerides and serum glucose. DLPC treatment also decreases hepatic steatosis and improves glucose homeostasis in two mouse models of insulin resistance. Both the antidiabetic and lipotropic effects are lost in liver-specific *Lrh-1* knockouts. These findings identify an LRH-1 dependent phosphatidylcholine signalling pathway that regulates bile acid metabolism and glucose homeostasis.

Increased fat accumulation in the liver—steatosis—is tightly correlated with insulin resistance and type 2 diabetes[6]. Modestly raised bile acid levels decrease steatosis[7]. Loss of the nuclear receptor LRH-1 decreases bile acid levels[1,2], indicating that an LRH-1 agonist could increase them and improve fatty liver. In screens of a number of different phosphatidylcholine (PC) and other phospholipid species for effects on human LRH-1 transactivation, dilauroyl PC (DLPC; C12:0/C12:0) and diundecanoyl PC (DUPC; C11:0/C11:0) showed strong stimulation (Fig. 1a). Comparable responses were not observed with closely related PCs differing in acyl chain length by only a single methylene group, or with any other C12:0/C12:0 phospholipid species (Supplementary Fig. 1a–c).

DLPC and DUPC, but not the bile acid chenodeoxycholic acid (CDCA) or the more conventional phospholipid dipalmitoyl PC (DPPC; C16:0/C16:0), also activated the synthetic LRH-1 reporter in several other cell lines, including CV-1 and HEK293T cells (data not shown), and specifically increased basal LRH-1 transactivation of the native mouse SHP promoter[8] by approximately twofold in HeLa cells (Supplementary Fig. 2a). DLPC and DUPC also induced a similar response with the OCT4 promoter, which was dependent on both LRH-1 cotransfection and an intact LRH-1 response element[9] (Supplementary Fig. 2a). DLPC and DUPC responsiveness was not altered in mutant LRH-1 derivatives previously shown to inactivate responses to LRH-1 phosphorylation[10] or sumoylation[11], but was strongly decreased by mutations shown to block phospholipid binding[4] (Supplementary Fig. 2d).

Mouse and human LRH-1 showed essentially equivalent responses to DLPC and DUPC, and both DLPC and DUPC also activate the close LRH-1 relative SF-1 (also known as NR5A1; Supplementary Fig. 2). The LRH-1 responses were dose dependent (Supplementary Fig. 2c). Neither DUPC nor DLPC showed significant activation of any of a number of additional nuclear receptors outside of the NR5A subgroup (Supplementary Fig. 2b). In particular, DLPC and DUPC failed to activate PPARα, which was recently reported to be specifically bound and activated by 1-palmitoyl-2-oleoyl (C16:0/C18:1) PC[12], and C16:0/C18:1 PC failed to affect LRH-1 transactivation (Supplementary Fig. 1a). DLPC rapidly induced expression of the LRH-1 target CYP8B1 in the C3A derivative of HepG2 cells (Supplementary Fig. 3a). This response as well as CDCA repression of CYP8B1 expression and transactivation of a synthetic LRH-1 reporter plasmid was specifically compromised in cells transfected with LRH-1 short interfering RNA (siRNA; Supplementary Fig. 3b, c).

We used the mammalian two-hybrid assay and a simple GST pull-down approach to initially test the predicted function of DLPC and DUPC as LRH-1 agonist ligands. In the mammalian two-hybrid analysis, interaction of a VP16–human LRH-1 ligand-binding-domain fusion with a second fusion of the Gal4 DNA-binding domain to the nuclear receptor interaction domain of the coactivator SRC-3 (also known as NCOA3) was unaffected by vehicle, CDCA or DPPC, but was stimulated by either DUPC or DLPC (Supplementary Fig. 4a). *In vitro*, SRC-3 protein did not bind to GST alone but showed a significant basal interaction with a GST–LRH-1-ligand-binding-domain fusion protein, as expected[4]. DLPC and DUPC further increased binding of the coactivator by approximately 3 fold, but vehicle, CDCA, or any of a number of other PC species, including DPPC, had little or no effect (Supplementary Fig. 4b). DLPC also unexpectedly but specifically decreased binding of an SRC-2 peptide to the LRH-1 ligand-binding domain with a half-maximum inhibitory concentration (IC_{50}) of approximately 500 nM, but DPPC had no effect (Supplementary Fig. 4c), and DLPC did not affect rosiglitazone binding to PPARγ (Supplementary Fig. 4d).

As a stringent test of specific binding, the purified bacterially expressed human LRH-1 ligand-binding domain was incubated with DLPC or DPPC at molar ratios of 1:1 or 1:5 (protein:PC), or with buffer alone, and the protein was then repurified to eliminate unbound lipids. Specifically bound lipids were extracted and compared to DLPC or DPPC by electrospray ionization mass spectrometry. Phosphatidylethanolamine (PE) and phosphatidylglycerol (PG) species with 16–22 carbon acyl chain lengths occupy the ligand-binding pocket in the buffer-treated control, with the most abundant peak corresponding to 16:1/18:1 PG (Fig. 1b). DLPC completely replaced these *Escherichia coli* phospholipids, even at an added lipid to protein molar ratio of only 1:1, but DPPC showed no detectable displacement, even at a ratio of 1:5 (Fig. 1b). On the basis of these functional and *in vitro* biochemical results, as well as the extensive structural studies demonstrating phospholipid binding to NR5A receptors[3–5,13,14], we conclude that DLPC and DUPC act *in vitro* as LRH-1 agonists. The functional results indicate that they may also act directly as agonists *in vivo*, although it remains unclear how they might transit the cell membrane and cytosol and enter the nucleus.

PCs are normal dietary nutrients that are efficiently absorbed in the small intestine, and we used the simple route of oral gavage to deliver cholic acid (CA), DLPC, DUPC and DPPC to C5BL/6 mice. These treatments had no apparent toxic effects and did not alter normalized

[1]Program in Developmental Biology, Baylor College of Medicine, Houston, Texas 77030, USA. [2]Department of Molecular and Cellular Biology, Baylor College of Medicine, Houston, Texas 77030, USA. [3]Department of Integrative Medical Sciences, Northeastern Ohio Universities Colleges of Medicine and Pharmacy, Rootstown, Ohio 44272, USA. [4]The Scripps Research Molecular Screening Center, The Scripps Research Institute, Scripps Florida, Jupiter, Florida 33458, USA. [5]Department of Biochemistry, Emory University School of Medicine, Atlanta, Georgia 30322, USA.

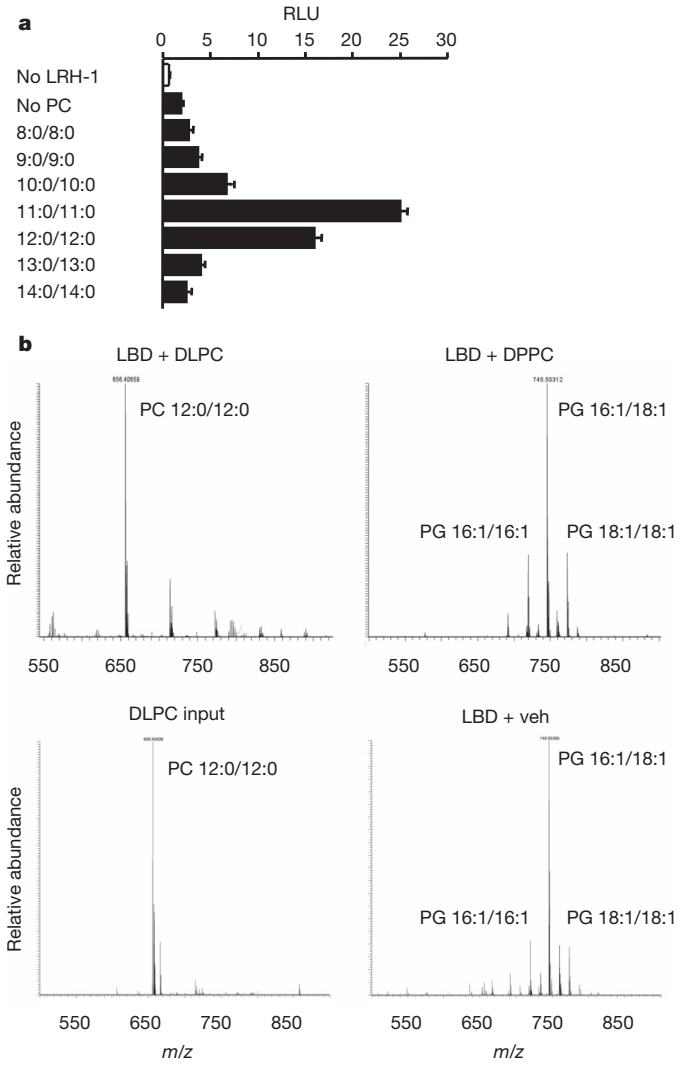

Figure 1 | DLPC activates and binds human LRH-1. a, HeLa cells were transfected with a human LRH-1 expression vector and a luciferase reporter and treated with 100 μM of indicated PCs. Error bars represent mean ± s.e.m. RLU, relative luciferase units. **b**, The human LRH-1 ligand-binding domain (LBD) was expressed and purified as described previously[5] and was incubated at molar ratios of 1:1 and 1:5 (human LRH-1 LBD:PC) with DLPC, DPPC or vehicle (veh) for two hours at 37 °C, and then repurified by size exclusion chromatography to remove unbound phospholipids. Bound lipids were analysed using electrospray mass injection mass spectrometry in the negative-ion mode. Results with DLPC (1:1), DPPC (1:5) and vehicle are shown, along with analysis of re-extracted DLPC; DLPC (1:5) and DPPC (1:1) incubations were very similar to those shown. The re-extracted DPPC peak is at 768.5, and is not detectable in any of the DPPC incubations.

liver weight (Supplementary Fig. 5a) or increase serum indicators of liver damage (Supplementary Fig. 5b). CA reduced expression of CYP7A1 and CYP8B1 and induced SHP, as expected, and DPPC was without significant effect (Fig. 2a). Both DLPC and DUPC significantly induced expression of CYP7A1, CYP8B1 and SR-B1, and repressed SHP (Fig. 2a). The substantial induction of CYP8B1, particularly by DLPC, is in accord with the opposite response in liver-specific *Lrh-1* knockouts[1,2], which otherwise show relatively limited alterations in gene expression or liver physiology. The decreased SHP expression is consistent with the induction of the bile acid biosynthetic enzymes, but was not expected based on the acute response of the isolated SHP promoter in HeLa cells (Supplementary Fig. 2a). Because SHP represses its own expression in the liver[8], it is possible that an initial inductive response is followed by an autoregulatory decrease. The induction of CYP7A1 and CYP8B1 is lost in liver-specific *Lrh-1* knockouts generated by infecting LRH-1 floxed (f/f) mice[2] with adenoviral Cre (Ad-Cre) expression vectors (Supplementary Fig. 6a, b).

These gene expression changes were associated with a modest but significant increase in the total bile acid pool and serum bile acid levels in DLPC- and DUPC-treated mice (Fig. 2b), consistent with the opposite effect in liver-specific *Lrh-1* knockouts[1,2]. These DLPC and DUPC effects were lost in Ad-Cre-mediated liver-specific knockouts (Supplementary Fig. 6c). Both CA- and DUPC/DLPC-treated mice showed significantly decreased serum non-esterized fatty acids (NEFAs) (Fig. 2b) and hepatic triglycerides (Fig. 2c), which were associated with decreased serum glucose in DUPC/DLPC-treated, but not CA-treated mice (Fig. 2b). Serum and hepatic cholesterol levels were unaffected (Fig. 2b, c). As anticipated based on the effective clearance of phospholipid-containing gut-derived chylomicrons by the liver, neither DLPC nor DUPC altered expression of SF-1 target genes in the adrenal gland (Supplementary Fig. 5c).

Prompted by the lipid and glucose effects in the normal mice, we focused on DLPC, a natural product, and treated insulin-resistant leptin-receptor-deficient *db/db* mice for 2 weeks by oral gavage, followed by a glucose tolerance test (GTT). An insulin tolerance test (ITT) was carried out after 1 week of additional treatment. Glucose homeostasis was improved in DLPC-treated mice, as shown by the GTT and ITT (Supplementary Fig. 7a), as well as lower fasting serum insulin levels (Supplementary Fig. 7e). DLPC treatment did not affect body weight or a number of other parameters, but decreased expression of the lipogenic transcription factor SREBP-1c (also known as SREBF1) and its downstream targets, and significantly lowered hepatic triglyceride levels in the *db/db* mice (Supplementary Figs 7b–f and 8).

To critically test the role of hepatic LRH-1 in these antidiabetic effects, wild-type *Lrh-1*$^{f/f}$ and liver-specific *Lrh-1*$^{-/-}$ mice generated using an albumin-Cre transgene (Supplementary Fig. 9a) were fed a high-fat diet to induce obesity and insulin resistance (diet-induced obesity (DIO)) for 15 weeks. Continuing on the diet, they were treated daily by oral gavage with vehicle or DLPC for 3 weeks, and glucose homeostasis was assessed by GTT and ITT. Loss of LRH-1 did not affect glucose homeostasis in the *Lrh-1*$^{-/-}$ DIO mice relative to the *Lrh-1*$^{f/f}$ DIO mice (Fig. 3a). As in the *db/db* mice, DLPC treatment substantially improved glucose homeostasis in the *Lrh-1*$^{f/f}$ DIO mice as indicated by GTT and ITT, and these responses were absent in the *Lrh-1*$^{-/-}$ DIO mice (Fig. 3a). The DLPC treated *Lrh-1*$^{f/f}$ DIO mice also had decreased fasting serum glucose and insulin levels, resulting in an 80% decrease in the homeostatic model assessment of insulin resistance (HOMA-IR) (Fig. 3b). Increased insulin sensitivity was confirmed using the hyperinsulinaemic–euglycaemic clamp, which showed both increased glucose disposal and markedly decreased hepatic glucose production in the DLPC-treated mice (Fig. 3c). Increased overall insulin sensitivity was also confirmed by increased insulin-dependent phosphorylation of the insulin receptor, IRS2 and AKT in the DLPC-treated *Lrh-1*$^{f/f}$ livers, but not *Lrh-1*$^{-/-}$ livers (Fig. 3d and Supplementary Fig. 9c).

Total body weight and food intake (Supplementary Fig. 9b), as well as weights of liver, reproductive fat pads, or brown fat did not differ between the *Lrh-1*$^{f/f}$ and *Lrh-1*$^{-/-}$ DIO mice. However, the livers of DLPC-treated *Lrh-1*$^{f/f}$ DIO mice were less pale and fatty, and decreased lipid deposition was confirmed both histologically and by direct measurement of hepatic triglyceride levels (Fig. 4a, b). NEFA levels were also decreased by DLPC in *Lrh-1*$^{f/f}$, but not *Lrh-1*$^{-/-}$ DIO livers and serum (Fig. 4b). Hepatic and serum bile acid levels were significantly increased by DLPC in the *Lrh-1*$^{f/f}$, but not the *Lrh-1*$^{-/-}$ DIO mice (Fig. 4b). DLPC significantly induced both CYP7A1 and CYP8B1 expression in the *Lrh-1*$^{f/f}$ mice, and this specific response was absent in the *Lrh-1*$^{-/-}$ mice (Supplementary Fig. 10a). The expression of additional bile-acid-related genes, including the biosynthetic CYP7B1 and CYP27A1 and the hepatic bile acid transporters BSEP (also known as ABCB11) and NTCP (also known as SLC10A1) was not significantly affected by DLPC treatment in *Lrh-1*$^{f/f}$ DIO mice (Supplementary Fig. 10a).

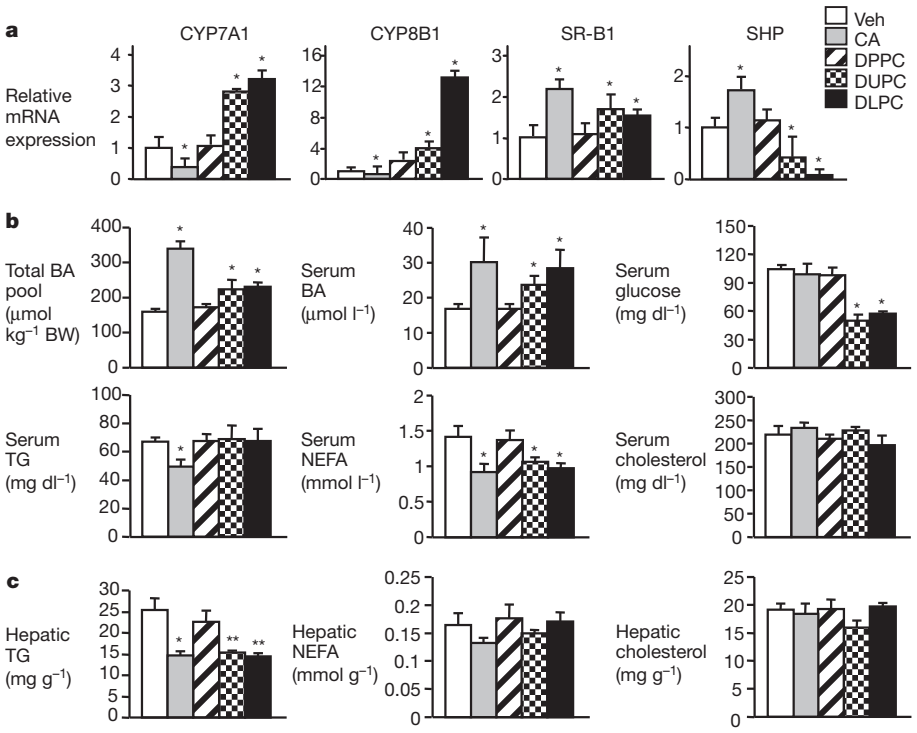

Figure 2 | DLPC and DUPC modulate expression of LRH-1 target genes in liver. a, Eight-week-old male C57BL/6 mice were challenged orally with vehicle (Veh), CA, DPPC, DUPC and DLPC for 3 days. Total liver RNA was isolated and prepared for the complementary DNA. Hepatic gene expression was determined using quantitative polymerase chain reaction (PCR). mRNA levels are relative to 36B4. **b**, Total bile acid (BA) pool and serum BA, glucose, triglyceride (TG), NEFA and cholesterol were measured in the same mice. **c**, Hepatic TG, NEFA and cholesterol were measured in the same mice. Error bars represent mean ± s.e.m. $*P < 0.05$, $**P < 0.01$ versus vehicle; $n = 5$ mice per group.

In accord with *db/db* results (Supplementary Fig. 8), there was little or no effect on hepatic expression of a number of glucose homeostasis and fatty acid oxidation genes (Supplementary Fig. 10d, e). However, DLPC markedly decreased expression of genes associated with *de novo* lipogenesis (Fig. 4c), including the lipogenic transcription factor SREBP-1c and its key downstream targets ACC-2, SCD-1 and FASN in *Lrh-1*$^{f/f}$ DIO mice (Fig. 4c). The beneficial effects of DLPC on glucose homeostasis and fatty liver in *Lrh-1*$^{f/f}$ mice fed a high-fat diet and infected with a control Ad–GFP vector were also lost in mice in which the *Lrh-1*$^{f/f}$ allele was deleted by Ad-Cre expression (Supplementary Fig. 11). Overall, we conclude that LRH-1 is required for the antidiabetic effects of DLPC. However, it remains to be determined whether its effects are a consequence of being a direct ligand for LRH-1, and it remains possible that DLPC activates an alternative signalling cascade or induces biosynthesis of an endogenous LRH-1 ligand.

Here we have identified DLPC as a specific agonist ligand for LRH-1 *in vitro*. Further studies will be needed to address the intriguing questions of whether phospholipid transfer proteins[15] facilitate its transport to the large and dynamic intranuclear pool of phosphatidylcholine[16], and whether DLPC is an endogenous LRH-1 agonist. The ligand responsiveness of LRH-1 is consistent with the identification of synthetic agonists that activate both LRH-1 and SF-1 (ref. 17). When expressed in an adrenal cell line, SF-1 is bound by a relatively low molecular weight form of phosphatidic acid with two saturated 14 carbon acyl chains, which acts as an agonist for SF-1 but not LRH-1 (ref. 18). Earlier results identified the sphingolipids sphingosine and lyso-sphingomyelin as potential endogenous antagonists of SF-1 transactivation[19]. DLPC does not activate other nuclear receptors, including PPARα or PPARγ, which have previously been reported to be activated by more conventional longer chain phospholipid species[12,20,21]. In the opposite direction, LRH-1 is not activated by conventional PC species, including the C16:0/C18:1 PC reported to specifically bind and activate PPARα in the liver[12]. Phospholipids are emerging as a structurally diverse class of highly specific nuclear receptor ligands.

The beneficial effect of DLPC on steatosis is associated with significantly decreased expression of the transcription factor SREBP-1c and its downstream lipogenic targets. At least two complementary mechanisms could contribute to this decrease. As SREBP-1c autoregulates its own expression[22], the reported functional antagonism of SREBP-1c transactivation by LRH-1 (ref. 23) could directly inhibit SREBP-1c promoter activity. As SREBP-1c expression is induced by insulin[24], the DLPC-dependent decrease in serum insulin should also decrease SREBP-1c messenger RNA. The combination of these two mechanisms could set up a positive regulatory loop in which the initial LRH-1-dependent repression of SREBP-1c expression would decrease steatosis and increase insulin sensitivity, resulting in a decrease in serum insulin. This decrease would then reinforce the decline in SREBP-1c expression and activity, further ameliorating fatty liver and thereby continuing a beneficial cycle (Supplementary Fig. 12). This essentially reverses the lipogenic vicious cycle to insulin resistance proposed previously by McGarry[25], and supported by more recent results with SREBP-1c[26].

These beneficial effects are probably complemented by an increase in fatty acid β-oxidation due to the decrease in acetyl-CoA carboxylase-2 (ACC-2) and its product, malonyl-CoA, which allosterically inhibits CPT-1a enzymatic activity and mitochondrial fatty acid uptake[27]. Decreasing ACC-2 activity in response to either specific antisense oligonucleotides[28] or activation of the nuclear receptor CAR[29] increases β-oxidation and has beneficial effects on both steatosis and insulin resistance. Because SCD-1 ablation also protects against hepatic steatosis by decreasing lipogenesis and increasing β-oxidation[30], reduced SCD-1 expression may also increase β-oxidation in response to LRH-1 activation.

We conclude that the identification of DLPC as a useful tool for analysis of LRH-1 function has uncovered an unexpected, LRH-1-dependent PC signalling pathway that can improve fatty acid and

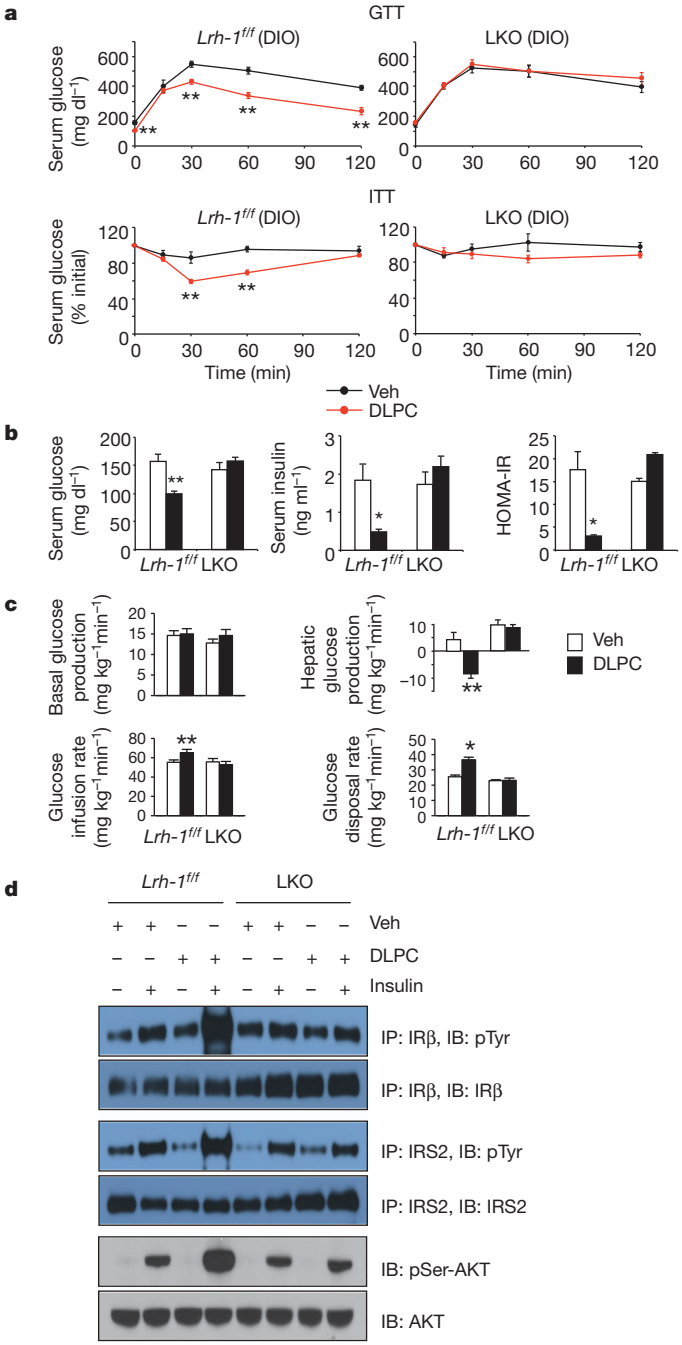

Figure 3 | DLPC improves glucose homeostasis in mouse models of insulin resistance. **a**, Glucose and insulin tolerance were assessed in *Lrh-1*$^{f/f}$ and *Lrh-1*$^{-/-}$ knockout (LKO) DIO mice 2–3 weeks after vehicle or DLPC treatment. **b**, Fasting serum glucose and insulin levels were measured in the same mice shown in **a**. HOMA-IR was calculated from fasting serum glucose and insulin levels. **c**, The high dose (10 mU kg^{-1} min^{-1}) hyperinsulinaemic–euglycaemic clamp (insulin dose of 10 mU kg^{-1} min^{-1}) was used to assess glucose homeostasis in *Lrh-1*$^{f/f}$ DIO mice after 3 weeks of vehicle or DLPC treatment. **d**, Hepatic insulin signalling was examined in *Lrh-1*$^{f/f}$ and LKO DIO mice 2 weeks after vehicle or DLPC treatment. Liver tissue homogenates from 3 mice per group were pooled and immunoprecipitation (IP) and immunoblotting (IB) were as indicated. Results are representative of three independent experiments. Error bars represent mean ± s.e.m. $*P < 0.05$, $**P < 0.01$ versus *Lrh-1*$^{f/f}$ DIO mice treated with vehicle; $n = 4$ mice per group.

glucose homeostasis. These studies indicate that DLPC is a promising therapeutic agent for the treatment of metabolic disorders, and we have initiated a human clinical trial to explore potential beneficial effects in prediabetic patients.

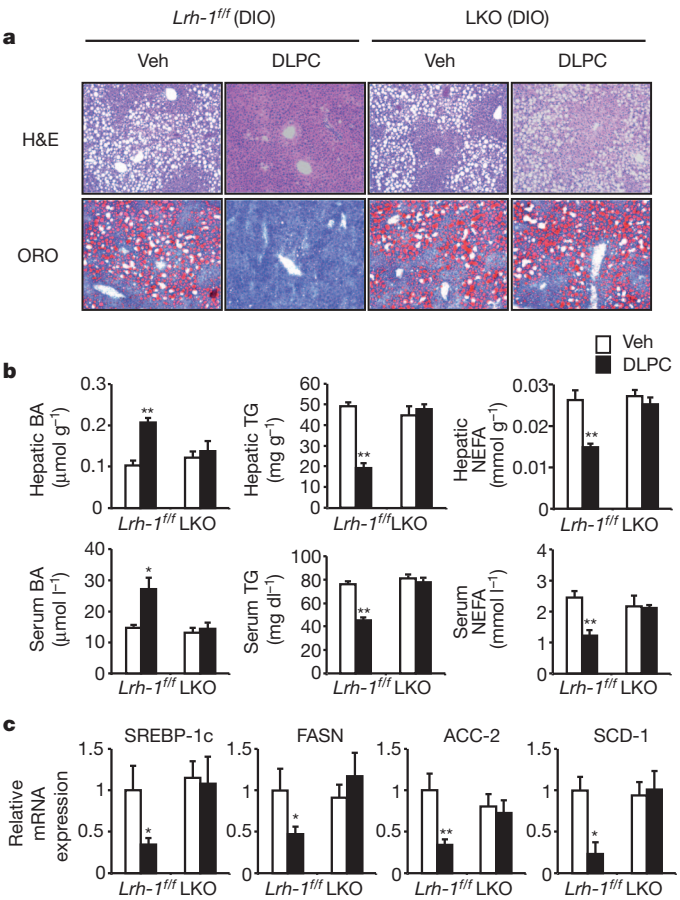

Figure 4 | DLPC reduces liver fat accumulation by suppressing lipogenesis. **a**, Liver sections from *Lrh-1*$^{f/f}$ and LKO DIO mice treated for 3 weeks with vehicle or DLPC were stained with haematoxylin and eosin (H&E) for general morphology or Oil Red O (ORO) for lipid accumulation. Original magnification, ×10. **b**, Hepatic and serum BA, TG and NEFA levels were measured in the same mice described in **a**. **c**, Lipogenic gene expression in the liver was determined using qPCR. mRNA levels are relative to 36B4. Error bars represent mean ± s.e.m. $*P < 0.05$, $**P < 0.01$ versus *Lrh-1*$^{f/f}$ DIO mice treated with vehicle; $n = 4$ mice per group.

METHODS SUMMARY

For transient transfection assays with HeLa, Cos-1 or C3A/HepG2 cells, candidate phospholipids dissolved in ethanol were added to cells for 24 h in medium containing 10% charcoal-treated FBS. Luciferase expression was assayed and normalized using β-galactosidase expression for transfection efficiency. Transfections were done in triplicate. For binding studies, the human LRH-1 ligand-binding domain, residues 291–541, was expressed as a maltose-binding protein fusion protein, cleaved and purified. It was incubated overnight with or without DLPC and specifically bound lipids were extracted with chloroform/methanol and analysed using electrospray mass injection mass spectrometry in the negative-ion mode to detect and identify phospholipids. LanthaScreen binding studies (Invitrogen) used full-length human LRH-1 and PPARγ. For short-term animal studies, C57BL/6 mice were orally gavaged with CA, DPPC, DUPC, or DLPC delivered in a standard vehicle every 12 h for a total of five treatments. Mice were killed 4 h after the final treatment on the morning of day 3. *Lrh-1* liver-specific knockout mice were generated as previously described[2]. For diabetes experiments, *db/db* mice were treated with vehicle or DLPC for 3 weeks. The GTT was performed 2 weeks after treatment. After an additional 1 week treatment, the ITT was performed. Eight-to-ten-week-old male control *Lrh-1*$^{f/f}$ or *Lrh-1*$^{-/-}$ mice were placed on a high-fat diet (45% kcal fat) for 15 weeks. The diet was maintained and mice were treated with vehicle or DLPC by oral gavage. GTT was performed in 18 h fasted mice after 2-week treatments. One week later, ITT was performed in *ad libitum* fed mice. Hyperinsulinaemic clamp (insulin dose of 10 mU kg^{-1} min^{-1}) was performed in the Diabetes and Endocrinology Research Center at the Baylor College of Medicine. All animal experiments were performed according to

procedures approved by the Baylor College of Medicine's Institutional Animal Care and Use Committee.

Statistics. Numbers of mice for each group used in experiments are indicated in the figure legends. Statistical analyses were performed with the two-tailed Student's *t*-test, and error bars represent means ± s.e.m. P value < 0.05 was considered statistically significant.

Full Methods and any associated references are available in the online version of the paper at www.nature.com/nature.

Received 19 March 2010; accepted 14 March 2011.

Published online 25 May; corrected online 29 May 2011 (see full-text HTML version for details).

1. Mataki, C. *et al.* Compromised intestinal lipid absorption in mice with a liver-specific deficiency of the liver receptor homolog 1. *Mol. Cell. Biol.* **27,** 8330–8339 (2007).
2. Lee, Y. K. *et al.* Liver receptor homolog-1 regulates bile acid homeostasis but is not essential for feedback regulation of bile acid synthesis. *Mol. Endocrinol.* **22,** 1345–1356 (2008).
3. Krylova, I. N. *et al.* Structural analyses reveal phosphatidyl inositols as ligands for the NR5 orphan receptors SF-1 and LRH-1. *Cell* **120,** 343–355 (2005).
4. Ortlund, E. A. *et al.* Modulation of human nuclear receptor LRH-1 activity by phospholipids and SHP. *Nature Struct. Mol. Biol.* **12,** 357–363 (2005).
5. Wang, W. *et al.* The crystal structures of human steroidogenic factor-1 and liver receptor homologue-1. *Proc. Natl Acad. Sci. USA* **102,** 7505–7510 (2005).
6. Cusi, K. Nonalcoholic fatty liver disease in type 2 diabetes mellitus. *Curr. Opin. Endocrinol. Diabetes Obes.* **16,** 141–149 (2009).
7. Watanabe, M. *et al.* Bile acids lower triglyceride levels via a pathway involving FXR, SHP, and SREBP-1c. *J. Clin. Invest.* **113,** 1408–1418 (2004).
8. Lee, Y. K., Parker, K. L., Choi, H. S. & Moore, D. D. Activation of the promoter of the orphan receptor SHP by orphan receptors that bind DNA as monomers. *J. Biol. Chem.* **274,** 20869–20873 (1999).
9. Gu, P. *et al.* Orphan nuclear receptor LRH-1 is required to maintain Oct4 expression at the epiblast stage of embryonic development. *Mol. Cell. Biol.* **25,** 3492–3505 (2005).
10. Lee, Y. K., Choi, Y. H., Chua, S., Park, Y. J. & Moore, D. D. Phosphorylation of the hinge domain of the nuclear hormone receptor LRH-1 stimulates transactivation. *J. Biol. Chem.* **281,** 7850–7855 (2006).
11. Chalkiadaki, A. & Talianidis, I. SUMO-dependent compartmentalization in promyelocytic leukemia protein nuclear bodies prevents the access of LRH-1 to chromatin. *Mol. Cell. Biol.* **25,** 5095–5105 (2005).
12. Chakravarthy, M. F. *et al.* Identification of a physiologically relevant endogenous ligand for PPARα in liver. *Cell* **138,** 476–488 (2009).
13. Li, Y. *et al.* Crystallographic identification and functional characterization of phospholipids as ligands for the orphan nuclear receptor steroidogenic factor-1. *Mol. Cell* **17,** 491–502 (2005).
14. Sablin, E. P. *et al.* Structure of SF-1 bound by different phospholipids: evidence for regulatory ligands. *Mol. Endocrinol.* **23,** 25–34 (2009).
15. Kang, H. W., Wei, J. & Cohen, D. E. PC-TP/StARD2: Of membranes and metabolism. *Trends Endocrinol. Metab.* **21,** 449–456 (2010).
16. Hunt, A. N. Dynamic lipidomics of the nucleus. *J. Cell. Biochem.* **97,** 244–251 (2006).
17. Whitby, R. J. *et al.* Identification of small molecule agonists of the orphan nuclear receptors liver receptor homolog-1 and steroidogenic factor-1. *J. Med. Chem.* **49,** 6652–6655 (2006).
18. Li, D. *et al.* Cyclic AMP-stimulated interaction between steroidogenic factor-1 and diacylglycerol kinase θ facilitates induction of CYP17. *Mol. Cell Biol.* **27,** 6669–6685 (2007).
19. Urs, A. N., Dammer, E. & Sewer, M. B. Sphingosine regulates the transcription of CYP17 by binding to steroidogenic factor-1. *Endocrinology* **147,** 5249–5258 (2006).
20. Lee, H. *et al.* Role for peroxisome proliferator-activated receptor α in oxidized phospholipid-induced synthesis of monocyte chemotactic protein-1 and interleukin-8 by endothelial cells. *Circ. Res.* **87,** 516–521 (2000).
21. McIntyre, T. M. *et al.* Identification of an intracellular receptor for lysophosphatidic acid (LPA): LPA is a transcellular PPARγ agonist. *Proc. Natl Acad. Sci. USA* **100,** 131–136 (2003).
22. Amemiya-Kudo, M. *et al.* Promoter analysis of the mouse sterol regulatory element-binding protein-1c gene. *J. Biol. Chem.* **275,** 31078–31085 (2000).
23. Kanayama, T. *et al.* Interaction between sterol regulatory element-binding proteins and liver receptor homolog-1 reciprocally suppresses their transcriptional activities. *J. Biol. Chem.* **282,** 10290–10298 (2007).
24. Shimomura, I. *et al.* Insulin selectively increases SREBP-1c mRNA in the livers of rats with streptozotocin-induced diabetes. *Proc. Natl Acad. Sci. USA* **96,** 13656–13661 (1999).
25. McGarry, J. D. What if Minkowski had been ageusic? An alternative angle on diabetes. *Science* **258,** 766–770 (1992).
26. Li, S., Brown, M. S. & Goldstein, J. L. Bifurcation of insulin signaling pathway in rat liver: mTORC1 required for stimulation of lipogenesis, but not inhibition of gluconeogenesis. *Proc. Natl Acad. Sci. USA* **107,** 3441–3446 (2010).
27. Kim, K. H. Regulation of mammalian acetyl-coenzyme A carboxylase. *Annu. Rev. Nutr.* **17,** 77–99 (1997).
28. Savage, D. B. *et al.* Reversal of diet-induced hepatic steatosis and hepatic insulin resistance by antisense oligonucleotide inhibitors of acetyl-CoA carboxylases 1 and 2. *J. Clin. Invest.* **116,** 817–824 (2006).
29. Dong, B. *et al.* Activation of nuclear receptor CAR ameliorates diabetes and fatty liver disease. *Proc. Natl Acad. Sci. USA* **106,** 18831–18836 (2009).
30. Dobrzyn, P. *et al.* Stearoyl-CoA desaturase 1 deficiency increases fatty acid oxidation by activating AMP-activated protein kinase in liver. *Proc. Natl Acad. Sci. USA* **101,** 6409–6414 (2004).

Supplementary Information is linked to the online version of the paper at www.nature.com/nature.

Acknowledgements We thank S. A. Kliewer and D. J. Mangelsdorf (UT Southwestern Medical Center) for the gift of *Lrh-1*$^{f/f}$ mice, A. J. Cooney for the OCT4 promoter constructs, C. Mills and D. Kuruvilla for experimental assistance, the Baylor College of Medicine Diabetes Endocrine Research Center (supported by NIH DK-079638 and USDA ARS 6250-52000-055) and the services of the Mouse Metabolism Core for hyperinsulinaemic clamp studies, and the current and previous members of the D.D.M. laboratory for discussions and technical support. Supported by NIH R01 DK068804, the Alkek Foundation and the Robert R. P. Doherty Jr—Welch Chair in Science to D.D.M., and NIH R01 CA134873 to P.R.G.

Author Contributions J.M.L. designed and executed the experiments, interpreted data and co-wrote the manuscript. Y.K.L. and J.L.M. helped with experiments. S.A.B. and P.R.G. performed the fluorescence binding experiments, and M.C.P. and E.A.O. performed the mass spectrometry experiment. D.D.M. supervised the design and interpretation of the experiments and co-wrote the manuscript.

Author Information Reprints and permissions information is available at www.nature.com/reprints. The authors declare no competing financial interests. Readers are welcome to comment on the online version of this article at www.nature.com/nature. Correspondence and requests for materials should be addressed to D.D.M. (moore@bcm.edu).

METHODS

Materials. Phospholipids were purchased from Avanti Polar Lipids; fatty acids, CA and CDCA from Sigma-Aldrich; cell culture media and supplements from Invitrogen; insulin from Eli Lilly and Co.; human LRH-1 antibody from R&D systems, antibody against IRβ, IRS2, pSer-AKT and AKT was from Cell Signaling Technology, anti-phosphtyrosine antibody from Millipore; Ad5-CMV–GFP or Cre virus was prepared by the Vector Development Laboratory at the Baylor College of Medicine.

Cell culture and transient transactivation assays. HeLa, Cos-1 and C3A/HepG2 cells were cultured in DMEM containing 10% FBS and 1% penicillin/streptomycin antibiotics. 70–80% confluent cells were replated into a 24-well plate with a 1:5 ratio 24 h before transfection. Cell culture media were changed 1 h before transfection (calcium phosphate method). At 16 h after transfection, candidate phospholipids dissolved in ethanol were added to cells for 24 h in medium containing 10% charcoal treated FBS. Luciferase expression was assayed and normalized using β-galactosidase expression for transfection efficiency. Transfections were done in triplicate. Plasmids used were pcDNA3 for empty vector (100 ng per well), LRH-1/SF-1 luciferase reporter (200 ng per well), actin-β-galactosidase for internal control (150 ng per well), human LRH-1 expression plasmid (100 ng per well), mutant human LRH-1 expression plasmids (100 ng per well, phosphorylation mutant: S238, 243A; sumoylation mutant: K270R; ligand-binding mutant: F342W, I426W), Oct4-PP luciferase reporter (200 ng per well), and Oct4-PP$_{mut}$ luciferase (200 ng per well). Expression plasmids for receptors (100 ng per well) and their cognate luciferase reporters (200 ng per well) used were: human T_3Rβ, TK-28T-Luc; human RXRα, TK-CRBPII-Luc; human RARβ, TK-DR5-Luc; mouse PPARα, mouse PPARδ, mouse PPARγ, TK-PPRE × 3-Luc; mouse FXRα, human FXRα, MMTV-TK-ECRE × 5-Luc; human LXRα, TK-LXRE × 3-Luc; human ERα, TK-ERE-Luc; mouse CAR, human CAR, human PXR, TK-DR4-Luc; mouse SF-1, mouse LRH-1, human LRH-1, LRH-1/SF-1 Luc. For mammalian two-hybrid assays, replated HeLa cells in a 24-well plate were transfected with VP-16 (50 ng per well), VP16-human LRH-1 ligand-binding domain (50 ng per well), Gal4-SRC-3 RID (100 ng per well), G5-TK-Luc (200 ng per well), and actin-β-galactosidase plasmids (150 ng per well). For siRNA experiments, C3A/HepG2 cells were maintained with MEM containing 10% FBS, 1 mM sodium pyruvate, 0.1 mM nonessential amino acids, and 1.5 g l^{-1} sodium bicarbonate. C3A/HepG2 cells were replated into either a 24-well plate for luciferase assay or a 6-well plate for target gene expression and then transfected with human LRH-1 (Dharmacon, ON-TARGETplus SMARTpool, L-003430-00; J-0003430-06: AUAUGAAUAGCCCA UUAUGUU, J-0003430-07: UAGCUGUCCAAAUUUCUCUUU, J-0003430-08: AGGAUUAAGAGCUCACUCCUU, J-0003430-09: UCACCUGAGACAUGGC UUCUU) or control siRNA pool (Dharmacon, si*CONTROL* non-targeting siRNA pool, D-001206-13-05; UAGCGACUAAACACAUCAA, UAAGGCUAU GAAGAGAUAC, AUGUAUUGGCCUGUAUUAG, AUGAACGUGAAUUGC UCAA) using FuGENE 6 (Roche); For the luciferase assay, C3A/HepG2 cells were transfected with LRH-1/SF-1 luciferase and actin-β-galactosidase along with the siRNA pool. Twenty-four hours later, ligands were added, and cells were harvested 24 h later. To check for knockdown, cell extracts were analysed by immunoblot using an antibody against human LRH-1.

***In vitro* binding assays.** GST pull-down was used to examine the interaction between human LRH-1 ligand binding domain and SRC-3 *in vitro* as described[4]. GST alone and GST human LRH-1 ligand-binding domain (amino acid residues, 185–541) were expressed in DH5α strain *E. coli* with 0.5 mM IPTG for 4 h and then purified with glutathione-sepharose beads (GE Healthcare). GST proteins were incubated overnight at 4 °C in 50 mM Tris-HCL (pH 7.6), 0.2% Tween-20, 100 mg ml^{-1} BSA and 300 mM NaCl with various phospholipids. Full-length [^{35}S]methionine-labelled SRC-3 proteins (2 μl) were added to each reaction and incubated for 2 h at 4 °C. Unbound and nonspecific proteins were removed by washing five times with the same buffer. Specifically bound proteins were eluted by treatment with SDS sample buffer, subjected to SDS–PAGE, and visualized by autoradiography. The amount of specifically bound SRC-3 proteins was determined by densitometry (Personal Densitometer SI; Molecular Dynamics).

Lanthascreen assays were as described by the manufacturer (Invitrogen) using full-length human LRH-1 and a fluorescein-tagged SRC-2 coactivator peptide, and PPARγ and Fluoromone[31].

For mass spectrometry, the human LRH-1 ligand-binding domain (LBD), residues 291–541, was expressed as a maltose-binding protein fusion protein, cleaved and purified as described previously[4]. The pure protein was stored in a final buffer containing 150 mM NaCl, 20 mM HEPES and 5% glycerol. For binding studies, DLPC or DPPC dissolved in ethanol was evaporated in a clean glass cuvette at 50 °C under a stream nitrogen gas. Two millilitres of buffer containing 150 mM NaCl, 20 mM HEPES (pH = 7.5) and 5% glycerol was added to the cuvette containing dried DLPC or DPPC and was sonicated until the solution was optically clear. Human LRH-1 LBD was then added to the DLPC or DPPC vesicles at a ratio of 1:1 or 1:5 (human LRH-1 LBD:PC). The mixture was incubated for one hour at 37 °C followed by 24 h at 11 °C. The human-LRH-1–lipid complex was then purified by size exclusion chromatography to remove unbound phospholipids. Protein purity was assed by SDS–PAGE. Bound lipids were analysed using electrospray mass injection mass spectrometry (ESI-MS) in the negative-ion mode to detect and identify phospholipids. Approximately 6 mg of human LRH-1 LBD or the human LRH-1-LBD–lipid complexes were extracted with a 2:1 chloroform/methanol solution, diluted in 200 ml chloromethylene and analysed by negative-ion ESI-MS on a Thermo LTQ FTMS using direct injection analysis with electrospray ionization. The high-resolution analyses were performed in the FTMS at a resolution of 100,000 at 400 *m/z*. The MS/MS experiments were done in the ion trap portion of the instrument with a mass selection of 3 AMU and a normalized collision energy of 30 V. The major phospholipid species were identified by accurate mass measurements and MS/MS via collisionally induced dissociation (CID), which yields product ions characteristic of the head groups and attached fatty acids.

Animal studies. C57BL/6 mice and *db/db* mice were purchased from Harlan laboratories. Eight-week-old male C57BL/6 mice were orally gavaged with CA, DPPC, DUPC, or DLPC at a dose of 100 mg kg^{-1} body weight, delivered in a standard vehicle for delivery of hydrophobic compounds (4:1 of PEG-400 and Tween-80) every 12 h for a total of five treatments. Mice were killed 4 h after the final treatment on the morning of day 3. Harvested tissues were immediately frozen in liquid nitrogen for molecular studies. Twelve-week-old male *db/db* mice were used for diabetes studies. *db/db* mice were given compounds (vehicle or DLPC, $n = 5$ mice per group) at the dose of 100 mg kg^{-1} day^{-1}. After 2 weeks of treatments GTT (1.5 g kg^{-1} intraperitoneal injection) was performed in 18 h fasted mice. Treatments were continued for an additional week, and ITT (2 U kg^{-1} intraperitoneal injection) was performed in *ad libitum* fed mice. Serum insulin levels were determined using Rat/Mouse Insulin ELISA Kit from Linco Research. *Lrh-1$^{f/f}$* mice[2] were maintained on mixed C57BL6/129 backgrounds and were given by the Kliewer/Mangelsdorf laboratory. In brief, 4-month-old male *Lrh-1$^{f/f}$* littermates were tail vein injected with either Ad5-CMV–GFP (3×10^9 p.f.u.) or Ad5-CMV-Cre (3×10^9 p.f.u.). For acute experiments, these mice were orally gavaged daily with each compound starting 2 weeks after adenovirus injection as described in C57BL/6 mice above. Liver-specific *Lrh-1* ablation (LKO) was also achieved by crossing *Lrh-1$^{f/f}$* mice with albumin-Cre transgenic mice obtained from the O'Malley laboratory at the Baylor College of Medicine. To confirm tissue-specific deletion of exon 5 of *Lrh-1*, genomic DNA was extracted from tail, liver and intestine, and PCR analysis was performed as shown previously[2]. For diabetes experiments, 8–10-week-old male control *Lrh-1$^{f/f}$* or LKO mice were placed on a high-fat diet (Research diets; 45% kcal fat) for 15 weeks. The diet was maintained and mice were treated with vehicle or DLPC (dose of 100 mg kg^{-1} day^{-1}) by oral gavage. GTT (2 g kg^{-1} intraperitoneal injection) was performed in 18 h fasted mice after 2-week treatments. 1 week later, ITT (1 U kg^{-1}, intraperitoneal injection) was performed in *ad libitum* fed mice. Glucose levels were analysed using a glucometer (LifeScan). Insulin resistance (HOMA-IR) was calculated as following: fasting glucose (mg dl^{-1}) × fasting insulin (μU ml^{-1}) / 405. Hyperinsulinaemic clamp (insulin dose of 10 mU kg^{-1} min^{-1}) was performed and calculated as described in our previous publication[32]. Ad–GFP- or Ad-Cre-infected *Lrh-1$^{f/f}$* mice fed the high-fat diet for 15 weeks were used for the diabetes study as shown above. Mice were housed in a temperature-controlled room in pathogen-free facilities on a 12 h light/dark cycle (07:00 on, 19:00 off) and had free access to water and standard chow diet. All animals received humane care according to the criteria outlined in the "Guide for the Care and Use of Laboratory Animals" prepared by the National Academy of Sciences and published by the National Institutes of Health.

RNA isolation and mRNA quantification. Total RNA was isolated from C3A/HepG2 cells or snap-frozen liver tissues using Trizol Reagent (Invitrogen) and prepared for the cDNA with QuantiTect reverse transcriptase (Qiagen). Hepatic gene expression ($n = 4$–5) was determined by qPCR using FastStart SYBR Green master (ROX) (Roche). mRNA levels were normalized by the 36B4 gene. Primer information can be provided upon request.

Serum and tissue lipid analysis. Blood was collected from the orbital plexus and transferred into gel/clot activator tubes (Terumo). Samples were centrifuged at 6,000*g* for 5 min to separate serum. To extract bile acids from liver or intestine, each tissue was weighed and homogenized in 75% ethanol. The homogenate was incubated at 50 °C for 2 h to extract bile acids and centrifuged at 6,000*g* for 10 min at 4 °C. The bile acid content of the supernatant was determined and normalized with tissue weight used. To extract other lipids, snap-frozen liver fragments were weighed and homogenized in nine volumes of PBS. Two-hundred microlitres of the homogenate was transferred into 1,200 μl of chloroform:methanol (2:1; v/v) mixture and mixed vigorously for 30 s. One-hundred microlitres of PBS was then added, and the resulting suspension was mixed vigorously for 15 s then centrifuged at 4,200*g* for 10 min at 4 °C. Two-hundred microlitres of the chloroform:methanol layer (bottom phase) was transferred into a tube and evaporated for dryness. The

dried lipid residue was resuspended in 100 µl of 1% Triton X100 in absolute ethanol for 4 h with constant rotation. Bile acids levels were measured using the bile acid L3K assay kit (Diagnostic Chemicals). Cholesterol and triglyceride levels were determined by assay kits from Thermo DMA. Free fatty acids were assayed using a kit obtained from WAKO Chemicals.

***In vivo* insulin stimulation and analysis of insulin signalling.** Mice were fasted overnight and injected intraperitoneally with insulin (1 U kg^{-1}) or PBS. Five minutes after injection, tissues were removed, frozen in liquid nitrogen, and stored at −80 °C until use. For protein extraction, tissues were homogenized in a cold lysis buffer (50 mM Tris-HCl, pH 7.4; 1% NP-40; 0.5% sodium deoxycholate; 150 mM NaCl; 1 mM EDTA) containing protease and phosphatase inhibitor cocktails (Roche). After homogenization, the tissue lysates were allowed to solubilize for 1 h at 4 °C with rotation, and then were centrifuged at 19,700*g* for 30 min at 4 °C. The supernatants were used for immunoprecipitations and immunoblot analyses of insulin signalling proteins.

Histology. Liver was removed and pieces were fixed in 10% (v/v) neutralized formalin solution (J. T. Baker), embedded in paraffin, sectioned at 5 µm, and stained with haematoxylin and eosin. For Oil Red O staining, frozen liver tissues embedded in O.C.T. compound (Tissue-Tek) were used. Histological analysis performed in the Comparative Pathology Laboratory at Baylor College of Medicine.

Statistics. Numbers of mice for each group used in experiments are indicated in the figure legends. Statistical analyses were performed with the two-tailed Student's *t*-test, and error bars represent means ± s.e.m. P value < 0.05 was considered statistically significant.

31. Vidović, D., Busby, S. A., Griffin, P. R. & Schurer, S. C. A combined ligand- and structure-based virtual screening protocol identifies submicromolar PPARγ partial agonists. *ChemMedChem* **6,** 94–103 (2011).
32. Ma, K., Saha, P. K., Chan, L. & Moore, D. D. Farnesoid X receptor is essential for normal glucose homeostasis. *J. Clin. Invest.* **116,** 1102–1109 (2006).